

# Semi-automatic laboratory equipment for reactive injection molding

A. S. Pouzada, A. M Brito, F. M. Oliveira, N. V. Dencheva, Z. Z. Denchev  
*IPC-Institute for Polymers and Composites/I3N, University of Minho, Guimarães, Portugal*

S. Lanceros-Méndez  
*Centre of Physics - GRF, University of Minho, Guimarães, Portugal*

**ABSTRACT** Traditional melt processing techniques limit in shape and thickness the parts of fiber-reinforced thermoplastic composites. Producing of thermoplastic hybrid composites through melt intercalation often results in heterogeneous products due to micron-scale agglomerations with a negative effect on the mechanical properties. The *in-situ* polymerization processes to form the matrix in polymer composites have proved to be a good approach toward the resolution of these issues. In the present work we report on the design and construction of a prototype semi-automatic laboratory equipment for reactive injection molding and its application for the preparation of various types of polyamide-6 based composites via *in-situ* activated anionic polymerization of  $\epsilon$ -caprolactam.

## 1 INTRODUCTION

Polymer composites with thermoplastic matrices (TPCs) comprising particulate or fibrous reinforcements are being used in steadily increasing number of diverse fields due to their excellent material performance, cost-effective production and manufacturing flexibility (Matabola et al, 2009). In principle, TPCs offer some important advantages over their thermoset counterparts such as higher toughness of the matrix, higher impact resistance, significantly shorter manufacturing cycles. In addition, TPCs can be welded (Stavrov & Bersee, 2005) and most importantly recycled (Steenkamer & Sullivan, 1998) while thermosets cannot. The latter feature becomes very important in view of the rigorous requirements for environmental protection imposed in most industrialized countries

TPC may be produced by either melt- or reactive processing techniques. The melt-processing techniques require melting of a thermoplastic polymer in the presence of the reinforcing component – fibrous, layered or particulate. The main disadvantage of melt processing toward TPC is the need for elevated processing temperatures and pressures, caused by the high melt viscosity of the matrix. In the case of fibrous reinforcements, proper impregnation of the fiber at a microlevel might be difficult and often results in products with a locally high void content. For TPCs with particulate and layered reinforcements, melt-processing often results in insufficiently fine dispersion of the reinforcing component or formation of agglomerates with negative influence on

the mechanical properties (Schaefer & Justice, 2007). The remark has to be made that melt-processed TPS frequently require various melting/recrystallization cycles (e.g., production of pellets with their subsequent extrusion or injection molding) whereby some thermoplastics such as polyamides and aromatic polyesters can slightly degrade due to their relatively high melting points in detriment to their mechanical properties.

In the reactive processing techniques the thermoplastic matrix is obtained through a polymerization process in the presence of the reinforcements. The polymerization has to produce high molecular weight linear polymer formed at sufficiently high conversions without the generation of unwanted by-products. From the suitable polymerization types most common is the ring-opening polymerization (ROP) [Bogov et al., 1981]. It is based on an ionic or condensation mechanism in which ring-shaped molecules are opened and transformed into high molecular weight polymers. n-Polyamides such as polyamide 6 (PA6) can be produced through activated anionic ROP (AAROP) of the inexpensive  $\epsilon$ -caprolactam (CL) without generating by-products. Polyesters as well as bisphenol-A polycarbonates and a number of high-performance polymers have been produced by condensation ROP (Brunelle et al, 1998).

Among the processes communicated to produce neat and reinforced PA6 reaction injection molding (RIM) and vacuum infusion (VI) seem to have potential for industrial application (van Rijswijk & Bersee, 2007). They are classical methods for the

preparation of thermoset composites attempted to be adapted for TPCs where the control on the chemistry of the matrix forming AAROP is still a big challenge.

The present work describes our recently developed prototype semi-automatic laboratory equipment for reactive injection molding that was used for the preparation of various TPC types via *in-situ* AAROP of  $\epsilon$ -caprolactam. Some initial studies on the properties of these TPCs are briefly reported.

## 2 EXPERIMENTAL PART

### 2.1 Sample preparation

The AAROP of CL in the presence of a commercial initiator (Dilactamate, DL) and activator (Bruggolen C20) using amounts that were previously found to be optimal (Dencheva et al, 2012). Two material batches were prepared that after mixing start to polymerize: a CL-activator batch and a CL-initiator batch. For the preparation of PA6 composites with particulate or layered reinforcement, equal amounts of the latter were introduced into each batch. Fibrous reinforcements (continuous filaments or textile structures) were impregnated with the mixture of the two batches directly in a heated closed mould. Due to the specific structure of the DL initiator, the anionically polymerizing systems in this work were less sensitive to inactivation of chain growth due to proton-donating species. It is worth noting that the AAROP was performed in the 160-175°C range, i.e., below the melting point of the resulting PA6 matrix (220°C, measured by DSC). Following polymerization, the composite product was demolded and further characterized.

This relatively complex reactive processing was performed in specially designed semiautomatic prototype equipment for reactive injection molding of nylons (NYRIM) schematically shown in Figure 1. The production cycle starts with liquefaction at 90°C of the CL-activator and CL-initiator batches and their separate introduction through the two inlets (Fig. 1B, pos. 3) into a steel block preheated to the same temperature. By simultaneous actuation of hydraulic cylinders C2 and C3 the two material batches are jet mixed. Then the cylinder C1 sprays the initiated and activated CL into the mold 2 preheated to the polymerization temperature. The mold is tightly closed previously actuating cylinder C4. After elapsing the pre-set reaction time (typically in the 20-30 min range) the mold cools down automatically to a preset temperature (typically 60°C) and opens through C4, thereby ejecting the composite plate (80x80x3mm). The maximum mold temperature is 250°C, and of the premixing camera – 200°C. Figure 2 shows the appearance of the NYRIM equipment.

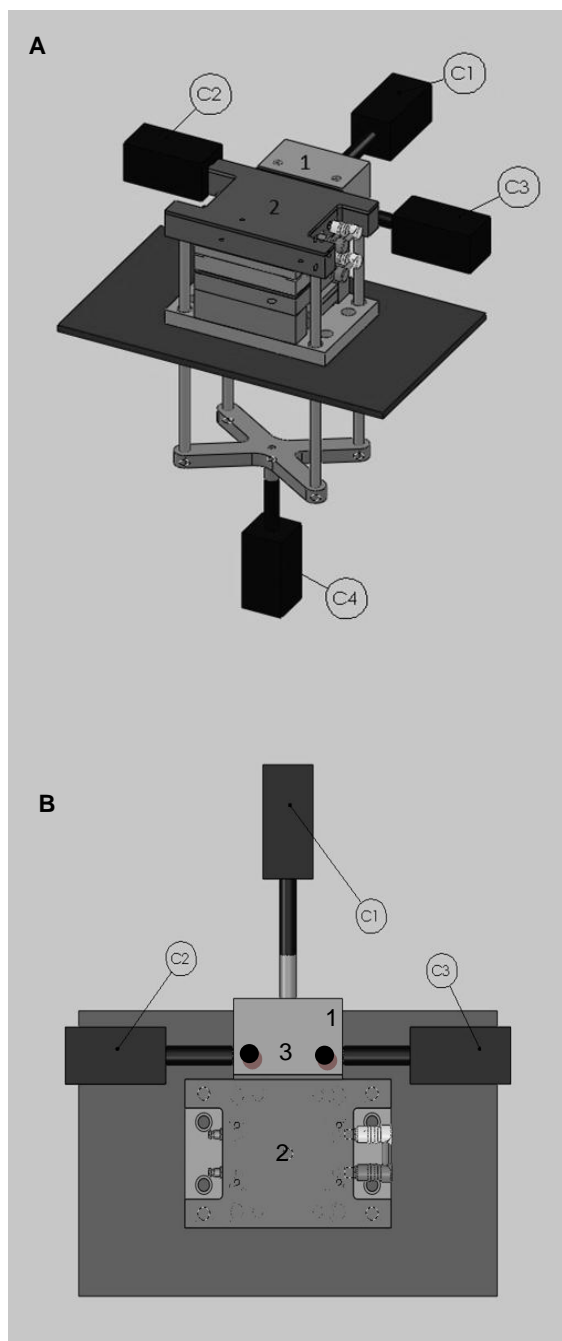


Figure 1. Prototype NYRIM processing machine concept: A – side view; B – top view. Legend: 1 – pre-heated camera for jet-mixing; 2 – the top plate of the mold; 3 – inlets for the two material batches of the pre-mixing camera; C1 – C4: hydraulic cylinders.

The figure shows also the configuration of the opened mold, the geometry of the composite plates and the aspect of selected composites samples.

Various PA6-based composite materials were prepared by means of the described procedure and equipment: pure anionic PA6, hybrid composites containing organically treated commercial nanoclay brands, carbon black and carbon nanofiber modified PA6, as well as glass-fiber reinforced PA6 using textile structures with different densities. The amounts and types of the reinforcements are summarized in Table 1. In all systems the AAROP was performed to high degree of conversion (96-99% determined by

means of Soxhlet extraction with methanol until constant weight.

to calculate the average and standard deviation values. The engineering stress was determined as the ratio of the tensile force to the initial cross section of the sample. The engineering strain was determined as the ratio of the sample gauge length at any time during drawing to that before drawing. The stiffness was calculated as the secant modulus from the stress–strain curves at 1% strain.

The impact resistance of the composite materials was studied by means of Charpy impact test according to DIN EN ISO 179. Standard test bars were cut out of the molded plates with a length of 80 mm and a cross-section of 3 mm x 10 mm that were notched to a depth of 2.54 mm having a radius of curvature of 0.25 mm. The bars are placed on supports 60 mm apart, resting of the narrower part, the notch being on the side furthest from the hammer. The notched impact strength was calculated as the impact energy absorbed relative to the test bar's cross-section. At least 5 bars from every composite were tested to determine the standard deviation values.

The TGA analyses were carried out in a TA Q500 gravimetric balance heating the samples from 50°C to 600°C at 10°C/min in nitrogen atmosphere.

The volume resistivity of the PA6-CB and PA6-CNF composites was obtained by measuring the characteristic I-V curves at room temperature using a Keithley 6487 picoammeter/Voltage source.

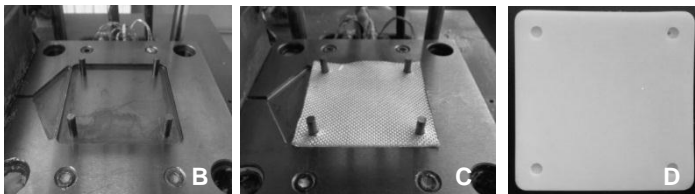
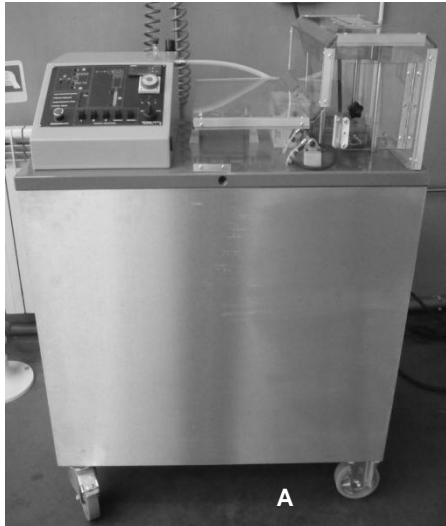


Figure 2. A - Prototype NYRIM processing machine – general view; B – configuration of the opened mold; C – the mold with the fibrous reinforcement; D – the finished composite plate.

Table 1. Description of the PA6-based composite materials of this study

Composite type	Designation	Reinforcement amount wt %
Neat anionic PA6	APA6	-
Nanoclay hybrids	PA6-CLO15	0.5; 1.0; 2.0; 3.0
	PA6-CLO20*	0.5; 1.0; 2.0; 3.0
Carbon black composites	PA6-CB	0.5; 1.0; 2.0; 3.0;
		5.0;
Carbon nanofiber	PA6-CNF	0.5; 1.0; 5.0
Glass fiber laminates	PA6-GF1**	
	PA6-GF2	20
	PA6-GF3	

\* CLO = Cloisite, organically treated montmorillonite clay

\*\* GF1-3 = glass fiber textile structures with low, medium and high densities

## 2.2 Characterization techniques

The tensile tests were performed with an Instron model 4505 tensile testing machine. The tests were carried out at  $23 \pm 2^\circ\text{C}$  with a standard load cell of 50 kN at a constant crosshead speed of 50 mm/min. From the different composite plates prepared in the NYRIM machine, standard specimens for tensile tests according to DIN 53504-S3 were cut out with a gauge length of 25 mm and a width of 4 mm. The sample thickness varied in the range of 2.5–3.0 mm. At least five specimens of each sample were studied

## 3 RESULTS AND DISCUSSION

### 3.1 Tensile tests results

Figure 3 shows the typical stress-strain curves of the various PA6-based composites studied. Table 2 shows the respective numerical data concerning the tensile behavior of the composites, as well as of the pure polyamide matrix materials obtained by anionic (APA6) or hydrolytic mechanisms (HPA6). APA6 was obtained in the NYRIM equipment by reactive molding at 160°C as were all the composites. HPA6 was compression molded from granules in a hot press under the same temperature. It can be seen that APA6 displays significantly lower strain at break ( $\epsilon_{br}$ ) values but higher modulus and stress at break ( $\sigma_{br}$ ) values than HPA6. Most probably this is due to the different crystalline structure of the two materials created by the different processing techniques: while APA6 structure is a result of solid state crystallization taking place simultaneously with the chain growth, hydrolytic PA6 is compression molded from granules. Most probably, the different processing techniques result in a different polymorph content that, as observed in previous studies, should lead to different tensile behavior (Dencheva et al, 2007).

Figure 1 and Table 2 show that particulate reinforcements such as CLO and CB as well as the CNF do not change significantly  $\sigma_{br}$  which is in the range

of 59-64 MPa, i.e., very close to that of the APA6 matrix but higher than HPA6. The montmorillonite-containing nanoclays CLO15 and CLO20 increased the modulus and acted differently on  $\varepsilon_{br}$ . These results are similar to the recently reported data on conventional HPA6/ montmorillonite-containing nanoclays (Motovilin et al., 2011), obtained however with larger amounts of clay that can be attributed to different homogeneity of the materials.

The carbon fillers CB and CNF increased both modulus and stress values, lowering at the same time the deformation at break. CB had some positive effect on the tensile behavior only at low concentration. Since the purpose of CB and CNF is to improve the composite conductivity, the fact that their addition is not in detriment of the mechanical performance is encouraging.

The tensile properties of the PA6-glass fiber laminates were clearly superior in comparison with either APA6 or HPA6. Keeping the same their weight percent in the composite, their reinforcing effect depended on the textile structure density, whereby the higher the density, the stronger the increase of the modulus or  $\sigma_{br}$  values.

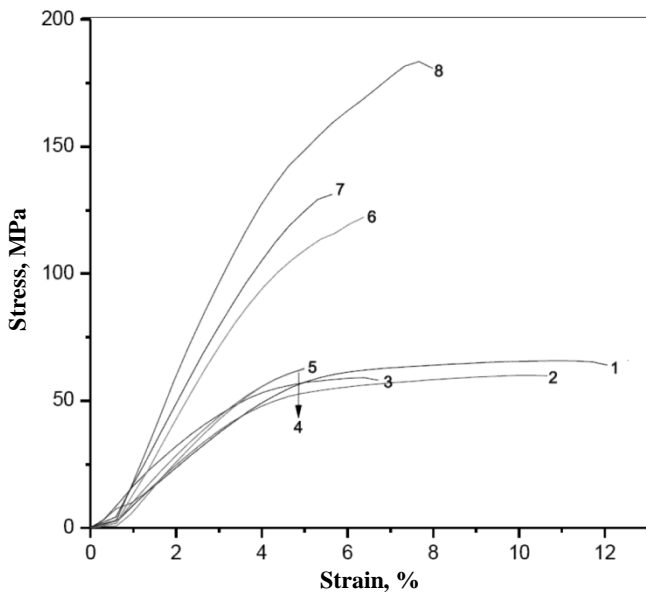


Figure 3. A – Typical stress-strain curves of the PA6-based composites produced in the NYRIM equipment. Curve designations 1-8 are according to the numbering in Table 2.

Table 2. Representative numerical results from the tensile tests

N° Sample	Filler wt. %	Young's modulus wt %	Stress at break $\sigma_{br}$ MPa	Strain at break, $\varepsilon_{br}$ %
- HPA6*	-	$1.0 \pm 0.1$	$47 \pm 2$	$70 \pm 18$
1 APA6	-	$1.6 \pm 0.2$	$66 \pm 2$	$11 \pm 3$
2 PA6-CL15	2.0	$1.7 \pm 0.2$	$60 \pm 2$	$10 \pm 2$
3 PA6-CL20	2.0	$2.0 \pm 0.3$	$59 \pm 1$	$6 \pm 1$
4 PA6-CB	0.5	$2.0 \pm 0.1$	$63 \pm 2$	$4 \pm 1$
5 PA6-CNF	2.0	$2.0 \pm 0.1$	$64 \pm 2$	$5 \pm 1$
6 PA6-GF1	20	$3.0 \pm 0.1$	$123 \pm 5$	$6 \pm 1$
7 PA6-GF2	20	$3.2 \pm 0.2$	$131 \pm 4$	$5 \pm 1$
8 PA6-GF3	20	$4.1 \pm 0.1$	$185 \pm 9$	$7 \pm 1$

\* Data from Dencheva et al., 2007.

### 3.2 Impact test results

Table 3 displays a comparison between the impact toughness of standard notched specimens prepared from the materials studied in a Charpy machine with a pendulum of 7.5 J at 23°C.

Table 3 Results from selected Charpy impact tests

Sample designation	Filler wt. %	Impact strength kJ/m <sup>2</sup>
HPA6*	-	7-15
APA6	-	68
PA6-CLO15	2.0	35
PA6-CLO20	2.0	34
PA6-GF1	20	143
PA6-GF2	20	158
PA6-GF3	20	201

\* Neat PA6 (Akulon K224) of DSM, The Netherlands

As expected, the glass fiber laminates displayed very significant improvement of the impact toughness that was directly proportional to the density of the textile structure. In the composites with layered clay reinforcements, the impact performance seems to be independent on the chemical treatment and gallery height, which are the main differences between CLO15 and CLO20 brands. The impact toughness of the respective composites is below that of the APA6 matrix but still much better as compared to the conventional HPA6. A similar impact behavior was found in hybrid composites of HPA6 containing 2.5 wt% of layered silicates from the bentonite group obtained by melt processing in a twin screw extruder (Debowska et al, 2007).

### 3.3 Resistivity test results

Table 4 compares the volume resistivity of various CB and CNF containing composites obtained in the NYRIM equipment. Depending on the concentration and type of the C-filler, the resistivity decreases by 3-4 orders of magnitude, i.e., from  $10^{12}$  (neat APA6) to  $10^8$ - $10^7$   $\Omega$ . This is enough for the transformation from isolator to antistatic or static dissipative material, thereby opening routes for applications in protection against spontaneous static discharge events.

Table 4 Results from the volume resistivity tests

Sample designation	Filler wt. %	Volume resistivity $\Omega$
APA6	-	$1.18^{12}$
PA6-CB	1	$9.77^{10}$
	2	$6.64^{09}$
	5	$8.72^{08}$
PA6-CNF	1	$5.18^{08}$
	2	$2.81^{07}$
	5	$1.75^{07}$

### 3.4 Thermogravimetric (TGA) tests

As stated above, in all composites of this study the conversion of  $\epsilon$ -CL monomer into APA6 during the reactive processing was quite high, in the range of 96-99%. This means that the various reinforcements did not inactivate or otherwise impede the AAROP process. However, since all APA6 composites were prepared in the presence of specific initiators and activators, it was quite important to control the amount of the volatile fractions formed at high temperatures. In the cases of particulate and layered reinforcements, it was also necessary to estimate the real concentration of these components. Figure 4 displays some typical TGA curves and Table 5 summarizes the data from these tests.

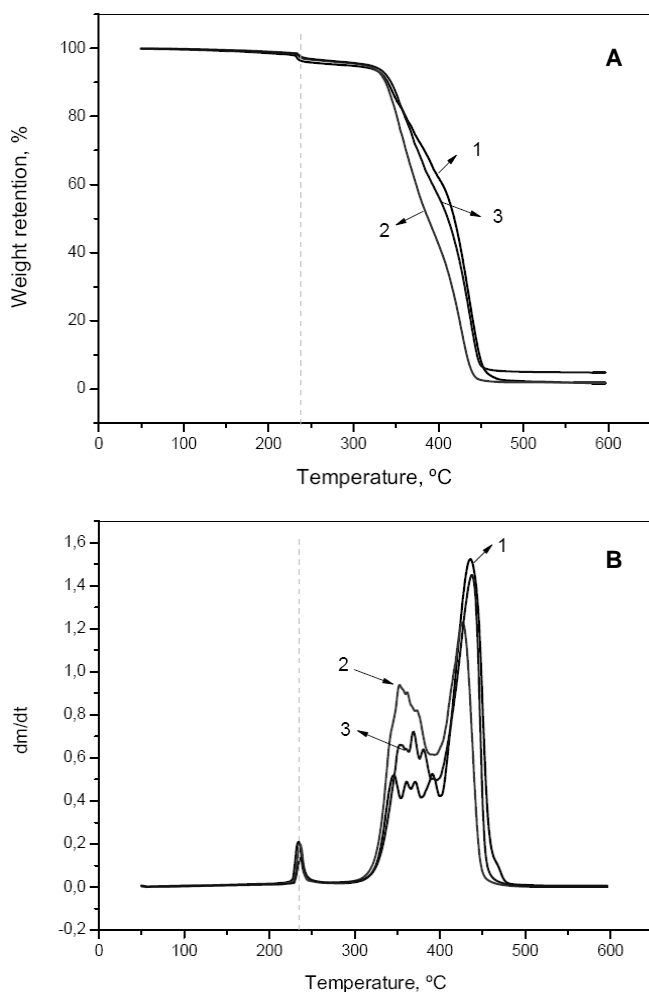


Figure 4. TGA curves in  $N_2$  atmosphere of selected composites: A – integral curves; B – first derivative curves. Legend: 1 – APA6; 2 – PA6-CLO15, 1 wt%.; 3 – PA6-CLO20, 1 wt%.

The TGA traces showed that all APA6-based composites in this study start losing mass above 230°C, i.e., higher than the melting point of the matrix. Up to 300°C the loss remains in the range of 3-4%. Intensive thermal degradation is observed around 350°C and 420°C, producing respectively 25-45% and 50-70% of the weight loss. The final residue at 600°C varies in the range of 1.5-6.0% depending directly on the amount of inorganic reinforcement. None of the Cloisite, CB, or CNF reinfor-

cements seems to be related to faster degradation in some of the three temperature ranges specified. Just the opposite, charges of 5% CB or CNF or 3% Cloisite reduce the weight losses in the range between 300-400°C from ca. 35% (neat APA6) to 20-25%. This is again indirect indication that the reactively molded plates are relatively homogeneous although further studies will be necessary to confirm this statement.

## 4 CONCLUSIONS

This work discloses some initial results related to the industrial application of the reactive processing of various types of APA6-based composites. It is based on the activated anionic polymerization of caprolactam in the presence of particulate, layered, fibrous and nanofibrous reinforcement carried out in specially designed, semiautomatic NYRIM prototype equipment. The processing technique and equipment used produced the respective composites with good yields and reproducibility. The results obtained suggest sufficient control on the chemistry of the process. The mechanical properties of the composites in tensile and impact modes are encouraging, especially as regards the APA6-fiber glass laminates. Composites with decreased resistivity useful for various advanced applications were also prepared.

The optimization of the mechanical and electrical properties of the APA6 composites passes through further detailed studies on the mutual relationship between: (i) the processing parameters (e.g., initiator/activator type and concentrations, temperature regimes during polymerization etc.); (ii) amount, type and treatment of the reinforcing components, and (iii) the nanostructure of the final composite including APA6 matrix polymorphism and transcrystallinity phenomena at the reinforcement-matrix interface.

## 5 ACKNOWLEDGEMENTS

NVD gratefully acknowledges the financial support of Fundação para a Ciência e Tecnologia, Portugal, under grant number SFRH/BPD/45252/2008 co-funded by FSE.

## 6 REFERENCES

- Bolgov, S.A., Begishev, V.P., Malkin, A.Y., Frolov, V.G. 1981. Role of the functionality of activators during isothermal crystallization accompanying the activated anionic polymerization of  $\epsilon$ -caprolactam. *Polymer Science USSR* 23:1485-1492.
- Brunelle, D.J., Krabbenhoft, H.O., Bonauto, D.K. 1993. Preparation of crystalline and solvent resistant polycarbonates via

ring-opening polymerization of cyclic oligomers. *Polymer Preprints USA* 34:73-744.

- Debowska, M., Dolega, J., Rudzinska-Girulska, J., Piglowski, J. 2008. Polyamide 6/layered silicate composites. *Acta Physica Polonica* 113(5):1322-1329.
- Dencheva, N., Denchev, Z., Oliveira, M.J., Funari, S.S. 2007. Relationship between crystalline structure and mechanical behavior in isotropic and oriented polyamide 6. *Journal of Applied Polymer Science* 103:2242-2252.
- Dencheva, N., Denchev, Z., Pouzada, A.S. On the structure-mechanical properties relationship of clay-reinforced PA6-based composites prepared by activated anionic polymerization of  $\epsilon$ -caprolactam. *Journal of Applied Polymer Science* (in press).
- Matabola, K.P., de Vries, A.R., Moolman, F.S., Luyt, A.S. 2009. Single polymer composites: a review. *Journal of Materials Science* 44:6213-6222.
- Motovilina, M., Denchev, Z., Dencheva, N. 2011. On the Structure-Properties Relationship in Montmorillonite-Filled Polyamide 6 Nanocomposites. *Journal of Applied Polymer Science* 120:3304-3315.
- Schaefer, D.W., Justice, R.S. 2007. How Nano are nanocomposites? *Macromolecules* 40: 8501-8517.
- Stavrov, D., Bersee, H.E.N. 2005. Resistance welding of thermoplastic composites - an overview. *Composites Part A: Applied Science and Manufacturing* 36:39-54.
- Steenkamer, D.A., Sullivan, J.L. 1998. On the recyclability of a cyclic thermoplastic composite material. *Composites Part B: Engineering* 29:745-752.
- van Rijswijk, K., Bersee H.E.N. 2007. Reactive processing of textile fiber-reinforced thermoplastic composites -an overview, *Composites Part A: Applied Science and Manufacturing* 38:666-681.